Hybrid nanoparticles as a new technological approach to enhance the delivery of cholesterol into the brain

Belletti Daniela, Grabrucker Andreas, Pederzoli Francesca, Menerath Isabel, Vandelli Maria Angela, Tosi Giovanni, Duskey Thomas Jason, Forni Flavio, Ruozi Barbara

PII: S0378-5173(18)30208-4
DOI: https://doi.org/10.1016/j.ijpharm.2018.03.061
Reference: IJP 17404

To appear in: *International Journal of Pharmaceutics*

Received Date: 11 January 2018
Revised Date: 28 March 2018
Accepted Date: 29 March 2018

Please cite this article as: B. Daniela, G. Andreas, P. Francesca, M. Isabel, V.M. Angela, T. Giovanni, D.T. Jason, F. Flavio, R. Barbara, Hybrid nanoparticles as a new technological approach to enhance the delivery of cholesterol into the brain, *International Journal of Pharmaceutics* (2018), doi: https://doi.org/10.1016/j.ijpharm.2018.03.061

Hybrid nanoparticles as a new technological approach to enhance the delivery of cholesterol into the brain

Belletti Daniela[1], Grabrucker Andreas[2,3], Pederzoli Francesca[1], Menerath Isabel[4], Vandelli Maria Angela[1], Tosi Giovanni[1], Duskey Thomas Jason[1], Forni Flavio[1], Ruozi Barbara[1#]

[1]Department of Life Sciences, University of Modena and Reggio Emilia, Modena, Italy
[2]Department of Biological Sciences, University of Limerick, Limerick, Ireland
[3]Bernal Institute, University of Limerick, Limerick, Ireland
[4]Institute for Anatomy and Cell Biology, Ulm University, Ulm, Germany

#Corresponding author

Dott. Daniela Belletti

Department of Life Sciences, University of Modena and Reggio Emilia

Modena, Via Campi 103, Italy

Tel.: +39 059 2058600

Email: daniela.belletti@unimore.it

ABSTRACT:

Restoration of the Chol homeostasis in the Central Nervous System (CNS) could be beneficial for the treatment of Huntington's Disease (HD), a progressive, fatal, adult-onset, neurodegenerative disorder. Unfortunately, Chol is unable to cross the blood-brain barrier (BBB), thus a novel strategy for a targeted delivery of Chol into the brain is highly desired.

This article aims to investigate the production of hybrid nanoparticles composed by Chol and PLGA (MIX-NPs) modified with g7 ligand for BBB crossing.

We described the impact of ratio between components (Chol and PLGA) and formulation process (nanoprecipitation or single emulsion process) on physico-chemical and structural characteristics, we tested MIX-NPs in vitro using primary hippocampal cell cultures evaluating possible toxicity, uptake, and the ability to influence excitatory synaptic receptors. Our results elucidated that both formulation processes produce MIX-NPs with a Chol content higher that 40%, meaning that Chol is a structural particle component and active compound at the same time. The formulation strategy impacted the architecture and reorganization of components leading to some differences in Chol availability between the two types of g7 MIX-NPs. Our results identified that both kinds of MIX-NPs are efficiently taken up by neurons, able to escape lysosomes and release Chol into the cells resulting in an efficient modification in expression of synaptic receptors that could be beneficial in HD.

1) Introduction:

Efficient delivery of cholesterol (Chol) has recently received considerable attention for its chances to succeed in the treatment of Huntington disease (HD) (Valenza et al., 2010; Zuccato et al., 2010). HD is an adult-onset, neurodegenerative disorder characterized by cell loss mainly in the striatum and cortex, and caused by an abnormal repetition of three DNA bases (Cytosine, Adenine and Guanine) in the gene encoding the huntingtin protein (htt). Among others, mutant htt has effects on sterol regulatory element binding proteins, which results in lower Chol levels in affected areas of the brain (Block et al., 2010).

The brain Chol is completely from endogenous source (local syntheses) being peripheral Chol unable to pass the blood-brain barrier (BBB) (Dietschy and Turley, 2004). Thus, the reduction of Chol biosynthesis in HD brain is detrimental for neuronal function altering both the structure and integrity, remodeling synapses, and consequently, synaptic transmission (Leoni et al., 2013; Valenza et al., 2007). The re-establishment of adequate Chol level in the brain appears as a promising approach in the treatment of HD where currently no effective therapies exist (Zuccato et al., 2010).

A number of strategies were developed to overcome BBB and to improve delivery of therapeutic agents to the brain. These approaches ranged from temporarily disrupting the barrier itself or modifying transported agents by chemical linkage to ligands able to enhance BBB drug permeability up to to deliver drugs directly into the brain through a variety of strategies which effectively bypass the BBB entirely (Gao 2016). More recently, to improve drug delivery to the brain, non-invasive techniques based on the use of nanocarriers able to loading drugs and modified on surface by conjugating antibodies or ligands received considerable attention (Hersh et al., 2016; Saraiva et al., 2016).

Recent *in vivo and in vitro* studies demonstrated that nanoparticles (NPs) based on FDA approved poly (D,L-lactide-co-glycolide) polymer (PLGA) and surface modified with a g7-glycopeptide (g7-NPs) are able to cross the BBB in a non-invasive way. This g7-glicopeptide conjugated onto NPs surface stimulates membrane curvatures and following endocytosis process of the whole system at BBB level, promoting the BBB crossing by multiple pathways (Tosi et al., 2011 a). Moreover, when loaded with drug (g7-NPs/Chol) are able to deliver Chol into the brain. Importantly, repeated systemic administration of g7-NPs/Chol rescued synaptic

communication, protected from cognitive decline and partially improved global activity in HD mice **(Valenza et al., 2015).** These results highlight the potential of g7-NPs/Chol in restoring brain Chol homeostasis with overall beneficial effects on HD pathology. Aiming at clinical translation some drawbacks must be overcome, especially the low drug-content (less than 1%), which force to repeated administrations and systemic accumulation of synthetic polymers. To overcome these possible limitations, we investigated a different approach, specifically designed to enable delivery of the therapeutic dose of Chol into the brain by a low number of administrations for a better patient-compliance.

This study aims to describe the formulation of new hybrid nanoparticles (named MIX NPs) based on a specific combination of polymer (g7-PLGA and PLGA) and Chol as formulative components. Hybrid nanoparticles were obtained applying nanoprecipitation (MIX-N) or single-emulsion (MIX-SE) techniques. Our study emphasizes the relationship between the nanoparticle composition and the formulation process with respect to the size, Chol content and nanoparticle stability. After the technological characterization both MIX-N and MIX-SE were tested *in vitro* on primary neuronal cells to investigate the tropism for brain cells and the toxicity.

Materials and Methods

2) Materials:

Poly(D,L-lactide-co-glycolide) (PLGA) (RG503H; 50:50 mol:mol, inherent viscosity 0.38 dL/g) was used as polymer (Boehringer-Ingelheim, Ingelheim am Rhein, Germany). According to the experimental titration results of the carboxylic end of the polymers, the MW of RG503H was calculated to be 11,000. Gly-l-Phe-d-Thr-Gly-l-Phe-l-Leu-l-Ser(O-β-d-glucose)-CONH2 (g7) was prepared as described previously and conjugated with PLGA to obtain g7-PLGA (Tosi et al., 2007)**.** The PLGA derivatization - yields (30-40 µmol peptide/g of polymer) were estimated by NMR from the relative peak area of the signals at 7.2-7.5 ppm, corresponding to the aromatic protons of the Phe present, and of the multiplet at 1.80–1.60 ppm corresponding to the protons of the methyl groups of the polymer. Rhod-PLGA was synthesized conjugating PLGA with Rhodamine B piperazine amide (Sigma-Aldrich, Milan, Italy) (Tosi et al., 2007)**.** Cholesterol (Chol), Pluronic-F68, and poly vinyl alcohol (PVA; 13-15000 Da, degree of hydrolysation 86–89 Mol%, viscosity at 4% w/v in water 3.5-4.5 cps) were purchased from Sigma Aldrich as well as the solvents (HPLC grade) used for analyses. Dulbecco's Modified Eagle Medium (DMEM), heat inactivated fetal bovine serum (FBS), and Dulbecco's Phosphate Buffered Saline (PBS) were purchased from Euroclone Celbio (Milan, Italy). Antibodies against MAP2 and GFAP were purchased from Novus Biological (Littleton, CO, USA) and Abcam (Cambridge, UK), respectively. Secondary antibodies Alexa and LysoTracker were obtained from Invitrogen (Life technologies, Darmstadt, Germany) and apoptosis/necrosis/healthy cell detection kit (Promokine) from PromoCell (Heidelberg, Germany). A MilliQ water system (Millipore, Bedford, MA, USA), supplied with distilled water, provided high-purity water (>18 MΩ). Unless otherwise indicated, all other chemicals were of analytical grade (Sigma Aldrich) and used without further purification.

3) Methods:

3.1 Preparation of nanoparticles

Nanoparticles composed by Chol and PLGA (MIX-NPs) were prepared by nanoprecipitation method (MIX-N) and by single emulsion technique (MIX-SE) using 50 mg of mixtures at different Chol:PLGA (w/w) ratio, i.e 1:1 (MIX _a), 1:0.4 (MIX _b), 1:0.25 (MIX _c) and 1:0.1 (MIX _d) (see supplementary **table S1**).

3.1.1 Nanoparticles obtained by the nanoprecipitation method (MIX-N)

To obtain MIX-N, the different Chol:PLGA mixtures were dissolved in acetone (4 mL). The organic phase was then added dropwise into 50 mL of a 0.5% (w/v) Pluronic-F68 aqueous solution at 45°C under magnetic stirring (1,300 rpm). After 10 min, the organic solvent was removed at 30°C under reduced pressure (10 mm Hg). The MIX-NPs were recovered and purified twice by an ultracentrifugation process carried out at 17,000 rpm for 10 min (4°C; Sorvall RC28S, Dupont, Brussels, Belgium) to remove the unformed material and the free surfactant fraction in the solution. The obtained MIX-N (MIX-N_a, MIX-N_b, MIX-N _c and MIX-N_d) were re-suspended in water (5 mL), stored at 4°C and used within a week.

NP-N (PLGA nanoparticles), were prepared as reference following the same procedure above described but using only PLGA (50 mg).

3.1.2. Nanoparticles obtained by the single emulsion method (MIX-SE)

In the single emulsion technique, the different Chol:PLGA mixtures were dissolved in dichloromethane (4 mL) and emulsified in 20 mL of 1% (w/v) PVA aqueous solution by sonication (Microson Ultrasonic cell disruptor, Misonix Inc. Farmingdale, NY, USA) (80W over 1 min) under cooling (5°C). Then, the O/W emulsion was stirred for at least 3 h (1,300 rpm; RW20DZM, IKALabortechnik, Staufen, Germany) at r.t. to allow the solvent evaporation. The MIX-SE (MIX-SE_a, MIX SE_b, MIX-SE_c and MIX-SE_d) were collected and purified by ultracentrifugation as previously described for MIX-N, and stored at 4°C before the use.

NP-SE (PLGA nanoparticles) were prepared as reference following the same procedure described for MIX-SE but using only PLGA (50 mg).

3.1.3. Nanoparticles preparation for the *in vitro* studies

g7-MIX NPs (g7-MIX-N_a and g7-MIX-SE _a) used for the *in vitro* experiments were obtained as above reported but using a mixture of Chol (50%), PLGA (45%), and g7-PLGA (5%). Labelled g7-(Rhod)-MIX NPs (g7-(Rhod)-MIX-N_a and g7-(Rhod)-MIX-SE_a) were prepared as reported above but using a mixture of Chol (50%), PLGA (42.5%), g7-PLGA (5%), and Rhod-PLGA (2.5%) (supplementary **table S1**).

3.2 Evaluation of yield

The recovered MIX-N or MIX-SE suspension was freeze-dried (-60°C, $1 \cdot 10^{-3}$ mm/Hg for 48 h; LyoLab 3000, Heto-Holten, Allerod, Denmark) and the yield (Yield%) was calculate as follows:

Yield (%) = [(mg of freeze dried MIX-N or MIX-SE)/(mg PLGA+ mg Chol)] x 100

3.3 Physico-chemical characterization of nanoparticles

Mean particle size (Z-Average) and polydispersivity index (PDI) of the samples were determined using a Zetasizer Nano ZS (Malvern, UK; Laser 4 mW He–Ne, 633 nm, Laser attenuator Automatic, transmission

100–0.0003%, Detector Avalanche photodiode, Q.E. > 50% at 633 nm). Samples were diluted in PBS pH 7.4 at about 0.5 mg/mL. The results were also expressed as intensity distribution, i.e. the size 10% [D(10)], 50% [D(50)] and 90% [D(90)], below which all the MIX NPs are placed. The zeta potential (ζ-pot l) was measured using the same equipment with a combination of laser Doppler velocimetry and phase analysis light scattering (PALS). All data are expressed as means of at least three determinations carried out for each prepared lot (three lots for each sample).

The morphology of the samples was evaluated by atomic force microscopy (AFM) (Park Instruments, Sunnyvale, CA, USA) at about 20°C operating in air and in non-contact mode using a commercial silicon tip-cantilever (high resolution noncontact "GOLDEN" Silicon Cantilevers NSG-11, NT-MDT, tip radius 10 nm; Zelenograd, Moscow, Russia) with stiffness of about 40 Nm^{-1} and a resonance frequency around 160 kHz. A drop of each MIX-NPs suspension was diluted with distilled water (about 1:5 v/v) before application on a small mica disk (1 cm× 1 cm). After 2 min, the excess of distilled water was removed using a paper filter and the sample analyzed. Two kinds of images were obtained: the first is a topographical image and the second is indicated as "error signal". This error signal is obtained by comparing two signals: the first one representing the amplitude of the vibrations of the cantilever, and the second the amplitude of a reference point. The images obtained by this method show small superficial variations of the samples. Images were processed and analyzed using software from Gwyddion (Department of Nanometrology, Czech Metrology Institute, Brno, Czech Republic).

The internal structure/architecture of the samples was analyzed by scanning transmission electron microscopy (STEM). Briefly, a drop of a water-diluted suspension of the samples (about 0.03 mg/mL) was placed on a 200-mesh copper grid (TABB Laboratories Equipment, Berks, UK), allowed to adsorb, and the suspension surplus was removed by filter paper. All grids were analyzed using a Nova NanoSEM 450 (FEI, Oregon, USA) transmission electron microscope operating at 30 kV using a STEM II detector in Field free mode.

3.4 Residual of surfactant

The residual amount of surfactants (Pluronic-F68 or PVA) was determined by a colorimetric method based on the formation of the colored complex between two adjacent hydroxyl groups of surfactant and an iodine molecule(Joshi et al., 1979). Briefly, 1 mg of a freeze-dried MIX NPs sample was solubilized in 0.5 mL of dicloromethane. Then, 10 mL of distilled water were added and the organic solvent was evaporated at r.t. under stirring for 2 h. The suspension was filtered (cellulose acetate filter, porosity 0.45 µm, Sartorius, Florence, Italy) to obtain an aqueous solution (A).

To detect the Pluronic-F68 residual, 2 mL of the aqueous solution (A) were treated with 2 mL of 0.5% (w/v) $BaCl_2$ in HCl 1N and 0.5 mL of an aqueous solution of I_2/KI (0.05 M/0.15 M). The obtained solution was incubated at r.t. for 10 min in dark. Pluronic-F68 concentration was determined measuring the absorbance at 540 nm (Model V530, Jasco, Cremella, Italy) in comparison to a standard plot of Pluronic-F68 prepared under the same experimental conditions. Linearity was assumed in the range of 2-18 µg/mL (r^2=0.995). All data are expressed as the mean of at least three determinations.

To quantify the PVA residual, the aqueous solution (A) (1 mL) was treated with 0.5 M NaOH (2 mL) for 15 min at 60°C. The solution was neutralized with 1 N HCl (900 µL) and the volume adjusted to 5 mL with water. Then, a solution of I_2/KI (0.5 mL) (0.05 M/0.15 M) and water (1.5 mL) was added to 3 mL of a water solution of boric acid (0.65 M). PVA concentration was determined measuring the absorbance at 690 nm (Model V530, Jasco) after 15 min of incubation at r.t. in comparison to a standard plot of PVA prepared

under the same experimental conditions. Linearity was assumed in the range of 2-150 µg/mL (r^2=0.998). All data are expressed as the mean of at least three determinations.

3.5 Cholesterol content

To quantify the amount of Chol into MIX NPs, an exact amount of MIX NPs (1 mg) was dissolved in 0.5 mL of chloroform, followed by addition of 1 mL of isopropyl alcohol to precipitate the polymer. The mixture was vortexed (15 Hz for 1 min; ZX3, VelpScientifica, Usmate, Italy) and then filtered (polytetrafluoroethylene filter, porosity 0.20 µm, Sartorius). The amount of Chol in the sample was quantified by RP-HPLC using an HPLC apparatus comprised a Model PU980 pump provided with an injection valve with a 50 µL sample loop (Model 7725i Jasco) and an UV detector (UV975, Jasco). Chromatography separation was carried out on a Syncronics C18 (250x4.6 mm; porosity 5 µm; Thermo Fisher Scientific, Waltham, MA, USA) at r.t. and with a flow rate of 1.2 mL/min, operating in an isocratic mode using 50:50 v/v acetonitrile:ethanol as mobile phase. The solvents of the mobile phase were filtered through 0.45 µm hydrophilic polypropylene membrane filters (Sartorius) before their use. Chromatographic peak-areas of the standard solutions were collected and used for the generation of calibration curves. Linearity was assumed in the range of 18-300 µg/mL (r^2=0.995). All data are expressed as the mean of at least three determinations.

3.6 Differential scanning calorimetry (DSC) studies

Thermal analysis was performed to evaluate the potential interaction between PLGA and Chol using a DSC 200 PC (Netzsch, Selb, Germany). Briefly, about 4 mg of the samples [MIX NPs, physical mixtures PLGA:Chol, plain PLGA and plain Chol] were put in crimped aluminum pans (Netzsch) and heated at the rate of 5°C/min using dry nitrogen flow (20 mL/min). As the final temperature (190°C) was reached, the system was cooled by liquid nitrogen to 10°C and a second heating cycle started (5°C/min from 20 to 190°C). Indium (99.99%; Perkin Elmer, Norwalk, USA) (melting point 156.6 °C; ΔH_f 28.45 J g^{-1}) was used to check the instrument. All DSC analyses were run in triplicate. T_{onset} is chosen to identify transition temperature while the enthalpy of process represents the total area of peak between T_i (initial temperature) and T_f (final temperature) calculated from the instrument software.

3.7 In vitro experiments

3.7.1 Cell culture

Hippocampal cultures were prepared from rat (embryonic day 18) as before described (Grabrucker et al., 2009)**.** In brief, after preparation of hippocampi from rat embryos, dissociated hippocampal neurons were seeded on poly-l-lysine (0.1 mg/ml; Sigma-Aldrich) coated 10 cm petri dishes at a density of 3 x 10^6 cells/dish or 24 well plates with a density of 3 x 10^4 cells/well. Cells were grown in Neurobasal™ medium (Life Technologies), complemented with 2% B27 supplement (Life Technologies), 2 mM L-Glutamine (Life Technologies) and 1% penicillin/streptomycin (Life Technologies) and maintained at 37°C in 5% CO_2. All experiments were performed in compliance with the guidelines for the welfare of experimental animals issued by the Federal Government of Germany and by the local ethics committee of Ulm University (ID Number: O.103).

3.7.2 Treatment of primary neuronal cultures with MIX NPs

Eleven days after seeding (11 DIV), culture medium was replaced with fresh medium containing MIXs NPs

(nanoparticles were diluted just before the treatment). After 6 h, the medium containing MIXs NPs was removed and cells were analyzed or incubated in fresh medium devoid of MIX NPs until 24 h. Treatments were performed maintaining a constant amount of Chol, which is the active part of the structure. In more detail, 200 µg of Chol (corresponding to 0.45 mg of g7-MIX-N_a or g7-(Rhod)-MIX-N_a and 0.36 mg of g7-MIX-SE_a or g7-(Rhod)-MIX-SE_a) were used to treat 300,000 cells. The selected concentration of Chol was not toxic as previously reported (Belletti et al., 2016).

3.7.3 Immunocytochemistry

For immunofluorescence, hippocampal neurons were fixed with 4% paraformaldehyde (PFA) / 4% sucrose / PBS at 4°C for 20 min. After washing 3x 5 min with 1x PBS containing 0.2% Triton X-100 at r.t., blocking was performed with 10% FBS/ 1x PBS for 1 h at r.t. Subsequently, the samples were incubated with the primary antibody at r.t. for 2 h. After a 3x5 min washing-step with 1x PBS, incubation with the secondary antibody coupled to Alexa488, Alexa568 or Alexa647 followed for 1 h. Cell nuclei were counterstained with DAPI and coverslips subsequently mounted using Vecta Mount (Vector Laboratories, Burlingame, CA, USA). Fluorescence images were obtained with an upright Axioscope microscope equipped with a Zeiss CCD camera (16 bits; 1280x1024 ppi) using Axiovision software (Zeiss, Jena, Germany). Quantification was performed using ImageJ Freeware version V 1.51a downloaded from the NIH website (http://rsb.info.nih.gov/ij).

3.7.4 Determination of cell health

In order to determine cell death (apoptosis versus necrosis), primary hippocampal neurons from rat were seeded on a 24 well plate, and apoptosis and necrosis were assessed using the apoptotic/necrotic/healthy cells detection kit according to the manufacturer guidelines. Treatment with 70% EtOH was used as positive control.

3.7.5 Protein Biochemistry

To obtain homogenate from treated neuronal cultures, cells were lysed and homogenized in lysis buffer (150 mM NaCl, 1% Triton X- 100, 50 mM Tris–HCl, pH 8.0) containing protease inhibitor (Roche, Mannheim, Germany). Cell debris and nuclei were removed by centrifugation at 3,200 rpm for 10 min resulting in supernatant S1 (soluble fraction) and pellet P1 (membrane associated fraction). Subcellular fractions were isolated as described previously with minor modifications(Schmeisser et al., 2012). Protein concentration was determined by Bradford protein assay. Proteins were separated by SDS-PAGE and blotted onto nitrocellulose membranes (GE Healthcare, Freiburg, Germany). Immunoreactivity was visualized using HRP-conjugated secondary antibodies and the SuperSignal detection system (Pierce, Upland, USA). Quantitative evaluation of bands was performed using ImageJ. Three independent experiments were performed. The individual bands were selected and the integrated density was measured. Bands were normalized to β-actin and the ratios averaged and tested for significance.

3.7.6 Statistics

Statistical analysis was performed with SPSS version 20. All data are shown as mean ± SEM. For comparisons, one-way analysis of variance (ANOVA) was performed followed by post hoc tests for within group comparisons (Bonferroni test). Statistically significant differences are indicated in the figures or text by * $p \leq 0.05$, ** $p \leq 0.01$ and *** $p \leq 0.001$.

4. RESULTS

4.1 Nanoparticle formulation

Z-Average (nm), polydispersivity index (PDI), ζ-pot (mV), yield, residual surfactant and % of Chol and PLGA forming MIX-N and MIX-SE are shown in **Table 1**.

Dimension of MIX-NPs formed by nanoprecipitation (MIX-N) suffers from some initial composition of the mixture, with both mean diameter and polidispersity increased along with the amount of Chol used in the formulation. MIX-N_a, prepared with a mixture of Chol:PLGA 1:1 (w:w), showed a mean diameter (Z-Average) of about 220 nm, a D(90) of 678 nm and a PDI value of 0.26. The increase of Chol amount in the initial mixture (MIX-N_b; Chol:PLGA 1:0.4 w:w) produced a significant ($p<0.05$) increase of Z-Average (up to 320 nm), D90 (920 nm) and PDI (0.31). The hypothesis of an increasing trend in the size is sustained by the dimensions of MIX-N with a higher Chol ratio. In fact, the Z-Average increased up to 361 nm (PDI= 0.36) in MIX-N_d where the weight polymer ratio is strongly increased in favor of Chol with respect to PLGA (Chol:PLGA 1:0.1). As far as the nanoparticle composition, by use more Chol in the mixture of production, the final structure resulted enrich in sterol, however the amount of PLGA and Chol really present in the MIX-N do not correspond to the nominally ratio used in the NP preparation. Briefly, MIX-N_a (Chol:PLGA 1:1 w:w) resulted in a polymeric-based structures composed by about 38% of Chol, 50% of PLGA and 12% of residual surfactant while Chol:PLGA 1:0.4 w:w sample (MIX-N_b) were almost lipidic-based NPs showing a significant increase ($p<0.05$) of the Chol content (65%) and a decrease of PLGA (22%) along with a constant surfactant residual (13%). MIX-N_d (Chol:PLGA 1:0.1 w:w) can be considered lipidic nanoparticles, composed by more than 80% of Chol, an amount of PLGA lower than 10% and a surfactant residue of 12%. The Chol-PLGA ratio used impact also the final yield, resulting in about 50% in both MIX-N_a and MIX-N_b and progressively decreased with the decreasing of the PLGA amount, reaching about a 40% value in MIX-N_d (Chol:PLGA 1:0.1 w:w).

The same mixtures of Chol and PLGA were used in the single emulsion procedure (MIX-SE) where PVA replaces Pluronic-F68 as surfactant. Most of the chemical physical characteristics analyzed were not affected by the ratio of PLGA and Chol used: all the samples showed a monomodal and monodisperse population with a Z-Average of about 290 nm (PDI about 0.2). The final composition was independent from that of the initial mixture composition. Both MIX-SE_a and MIX-SE_b were characterized by a more constant Chol:PLGA ratio (about 1:1; 40-45% w/w of Chol and 45-50% w/w of PLGA), i.e. the MIX NPs composition did not change as the initial Chol:PLGA ratio was modified. The PVA residue was about 6% in MIX-SE_a and about 15% in the other MIX-SE (MIX-SE_b, MIX-SE_c, MIX-SE_d) prepared using the higher amount of Chol. The only parameter affected by the nominal ratio of PLGA was the final yield of MIX-SE which was 65% in MIX- SE_a and reaching 15% in MIX- SE_d (formed by the highest Chol:PLGA ratio).

For both MIX-N and MIX-SE series, the negative ζ-pot value (ranging from about −30 and – 15 mV) was due to the exposition of oxydrilic and carboxyilic free groups on the surface of PLGA and Chol molecules.

Sample	Method	Chol:PLGA weight ratio (theoretical)	Z-Aver. (±SD) [nm]	PDI (±SD)	Di(50) (±SD) [nm]	Di(90) (±SD) [nm]	ζ-pot (±SD) [mV]	Yield (%)	Content of Chol (%)	Content of PLGA (%)	Content of surfactant (%)	Chol:PLGA weight ratio (experimental)
NP_N	N a	0:1	190 (±11)	0,1 (±0,01)	197 (±10)	250 (±6)	-27 (±1)	88 (±1)		91 (±3)	9 (±4)	

MIX-N_a		1:1	222 (±14)	0,26 (±0,05)	235 (±9)	678 (±86)	-24 (±3)	51 (±1)	38 (±5)	52 (±2)	10 (±2)	1:1.6
MIX-N_b		1:0.4	321 (±21)	0,31 (±0,07)	325 (±22)	920 (±162)	-22 (±4)	49 (±7)	65 (±3)	22 (±2)	13 (±2)	1:0.3
MIX-N_c		1:0.25	330 (±27)	0,32 (±0,07)	325 (±30)	1098 (±712)	-18 (±2)	50 (±4)	74 (±4)	11 (±3)	15 (±3)	1:0.15
MIX-N_d		1:0.1	361 (±22)	0,36 (±0,06)	359 (±24)	2245 (±88)	-21 (±3)	41 (±3)	81 (±1)	7 (±2)	12 (±3)	1:0.09
NP-SE	Single Emulsion	0:1	203 (±11)	0,12 (±0,02)	215 (±10)	340 (±8)	-24 (±1)	80 (±2)		94 (±2)	6 (±5)	
MIX-SE_a		1:1	286 (±16)	0,19 (±0,01)	283 (±10)	494 (±44)	-25 (±1)	62 (±2)	44 (±2)	50 (±2)	6 (±3)	1:1.1
MIX-SE_b		1:0.4	291 (±4)	0,22 (±0,03)	307 (±11)	542 (±77)	-19 (±3)	47 (±11)	40 (±7)	46 (±7)	14 (±4)	1:0.9
MIX-SE_c		1:0.25	283 (±9)	0,19 (±0,06)	284 (±11)	481 (±31)	-21 (±3)	28 (±7)	41 (±6)	44 (±7)	15 (±3)	1:0.9
MIX-SE_d		1:0.1	282 (±12)	0,13 (±0,03)	298 (±12)	529 (±24)	-13 (±2)	18 (±4)	39 (±2)	44 (±4)	17 (±4)	1:0.9

Table 1: Physico-chemical characterization of MIX NPs: Z-Average, PDI (polidispersivity index) and Zeta potential (ζ-pot) of MIX NPs after the purification process are shown. Content of Chol, PLGA and surfactant refers to weight of component with respect to 100 mg of total formulation recovered after the purification process.

4.2 Structural characterization:

4.2.1 Morphology

AFM and TEM were used to study only the morphology and structure of MIX-N_a, MIX-N_b, MIX-SE_a and MIX-SE_b (**Fig. 1**).

MIX-N_a were spherical and well-defined nanoparticles. Under AFM observation, they collapsed on the mica surface becoming flat structures with heights (H) not correlate to the diameters (ratio between diameter and height frequently about 6.5). TEM analyses revealed alterations of electron density related to differences in thickness likely associated to the hybrid structure of the matrix (Egerton, 2005)**.**

Both microscopic techniques allow to pointed out the effect on the Chol:PLGA ratio on the MIX-N stability. Particularly, AFM showed the collapsed unformed materials on mica surface that embedded aggregates of MIX-N_b in which a high amount of Chol was recovered (65% of MIX-N_b vs 38% of MIX-N_a). In this sample, TEM confirmed the presence of large amounts of un-formed materials both as continuous film enveloping the nanoparticles and non-electron dense spherical lipidic discs.

MIX-SE_a, notwithstanding some aggregations occurring after deposition on mica, is featured by well-defined particle populations, showing a good correlation between diameters and heights (diameter/height ratio of about 3). TEM analyses confirmed the presence of spherical and electron dense structures.

In contrast, MIX-SE_b were difficult to analyze with AFM as they showed high amounts of collapsed material that disrupts the tip approach. It is possible that the high amount of residual PVA in MIX-SE_b (14 % vs 6% of MIX-SE_a), probably adsorbed on surface, rapidly desorbed during deposition and dehydration (when occurred), produces a layer upholstering the nanoparticle surface. MIX-SE_a aggregates were easily detected using TEM analyses.

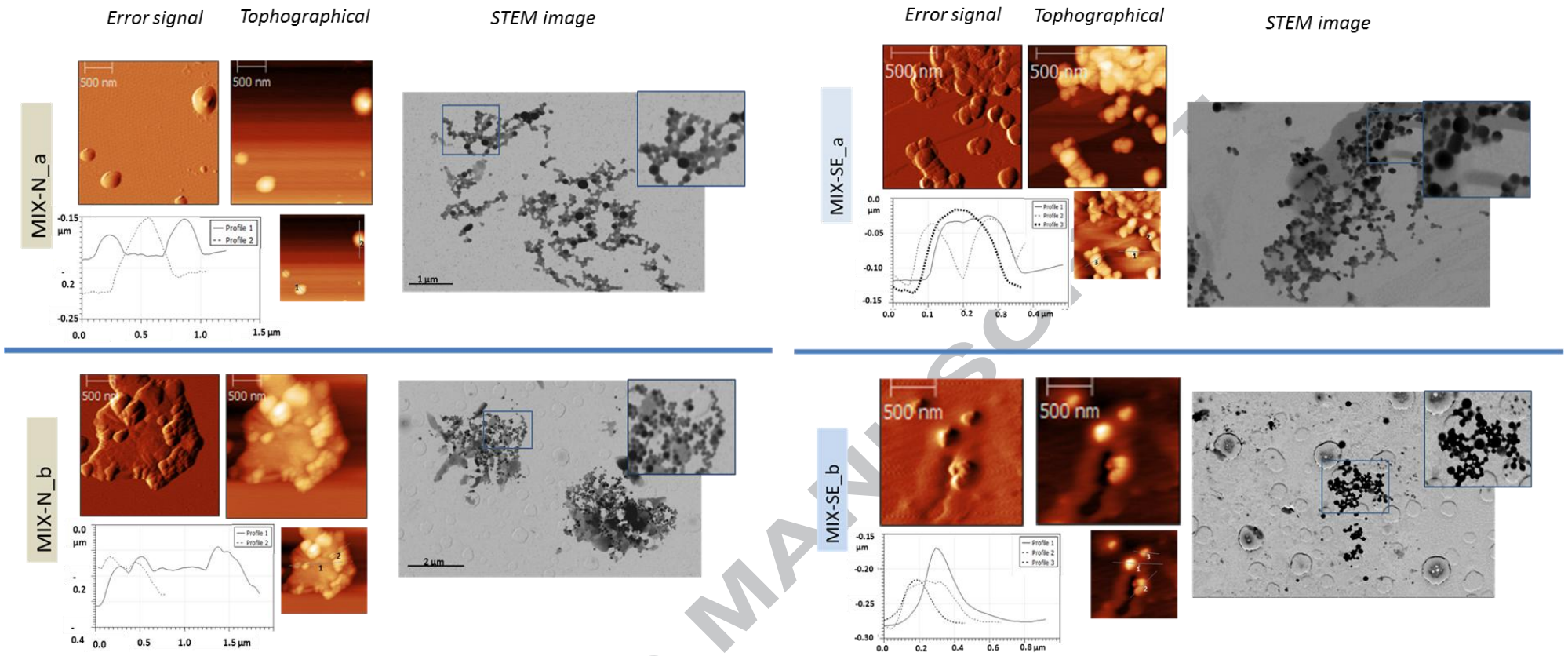

Fig. 1. Microscopic characterization of MIX NPs samples. Each panel reports a combination of AFM and TEM of the sample; left: AFM images (error signal, thopographical images with the related analyses of profiles) are reported- right: STEM images and related magnification.

4.2.2 DSC analyses

Fig. 2 shows the DSC curves of the components forming MIX NPs (PLGA, Chol, PVA, Pluronic-F68), of physical mixtures Chol:PLGA and of MIX-N_a, MIX-N_b, MIX-SE_a, and MIX-SE_b. All the samples underwent a heating run followed, after a cooling cycle, by a second heating run. The transition temperature (T_{onset}) and the enthalpy (ΔH, J/g) values associated with each transition were obtained through analysis of DSC-curves and are summarized in the supplementary **Fig. S1.**

The first heating run of the plain Chol (**Fig. 2 panel a1**) showed the polymorphic transition at 38±1°C (Bach and Wachtel, 2003) (ΔH =7±1 J/g) followed by the sharp endothermic peak at 151±2°C of the melting of the crystalline phase of Chol. After cooling, in the second heating run **(Fig. 2, panel a2**), the polymorphic crystalline transition of Chol did not appear, while the melting point was clearly visible. Plain PLGA showed an endothermic transition at 47±2°C, which corresponds to the typical Tg of polymer (**Fig. 2, panel a1).** In the second heating run, the Tg value of PLGA was slightly shifted (to about 49.0°C) probably as a result of the loss of water molecules occurring during the first heating run (**Fig. 2, panel a2**). [**15]** Pluronic-F68 showed the typical endothermic transition at 51±1°C, observed in both the first and second heating scan (**Fig. 2, panel a2**); PVA, a semi-crystalline polymer, showed an endothermic transition at 32±1°C, which corresponds to the typical Tg (Kapoor et al., 2015)**,** that did not appear in the second heating cycle.

The physical mixtures Chol:PLGA (**Fig. 2, panel b**) showed In the first heating cycle both the polymorphic crystalline transition and the melting point of Chol (38°C±1 and 151±2°C, respectively) that became less intense as the Chol:PLGA ratio decreased [(ΔH = 47 J/g in Chol-PLGA 1:0.1 (**Fig. 2, panel b-1, line a**) up to 3 J/g in Chol:PLGA 0.1:1 (**panel b-1, line f**)] owing to the decreasing amount of Chol. The PLGA transition (Tg) was only detected for polymer concentration was higher than 40% (Chol:PLGA 1:0.4, **panel b-1, line c**). During the second heating cycle, the thermograms of the physical mixtures Chol:PLGA 1:0.1 and Chol:PLGA 1:0.25 (**Fig. 2, panel b-2, lines a and b**) showed a faint endothermic transition in the range 30-50°C followed by the melting of Chol (151 ±2°C). Decreasing the Chol amount (**Fig. 2, panel b-2, lines c to f**) both transitions shifted towards a lower temperature. Enthalpy associated with the melting of Chol was reduced of about 30% in mixtures with 1:0.4 and 1:1 Chol:PLGA ratio and about 98% in Chol-PLGA 0.1:1 respect to the first heating cycle **(Fig. 2, panel b-2**) (**see supplementary Fig S1**).

These findings support literature data (Bettinetti and Mura, 1994; Chiou and Riegelman, 1971) and demonstrate that under controlled condition Chol and PLGA can produce a solid dispersion (by fusion method) where Chol can probably be distributed in the crust of the polymer.

The thermograms of MIX-N_a and MIX-N_b (**Fig. 2, panel c)** showed a large transition at about 50°C which changed during the second heating run in two peaks: the first at about 30°C could be associated to the polymorphic crystalline transition of Chol, and the second in the range of 46-49°C could be associated to Pluronic-F68. [**11]** The typical endothermic transition ascribable to the Chol melting occurred at 143±2°C in the first as well as the second heating cycle. The Chol enthalpy in the MIX-N_a and MIX-N_b agreed with the value estimated for the corresponding physical mixtures (about 20 J/g in MIX_N_a, and about 31 J/g in MIX-N_b). A small reduction in the enthalpy values (about 5%, **Fig. 2, panel c-2 and supplementary Figure S1**) was recorded in the second thermogram. Transitions related to PLGA were not clearly detectable in both the first and the second heating cycle.

In MIXs-SE only a faint signal at about 48°C was observed in the first heating cycle. The melting of Chol (147 ± 0.5°C) was clearly visible (25 J/g; similar to the value measured in mixture Chol:PLGA 1:1 w/w, **Fig. 2, line d, panel b**), this transition shifted through low temperature (142 ± 2°C) in the second run. The reduction of

enthalpy (about 20% with respect to the first run) as to that of the corresponding physical mixture (**line d, panel b**), suggests a miscibility of Chol and PLGA in MIX-SE.

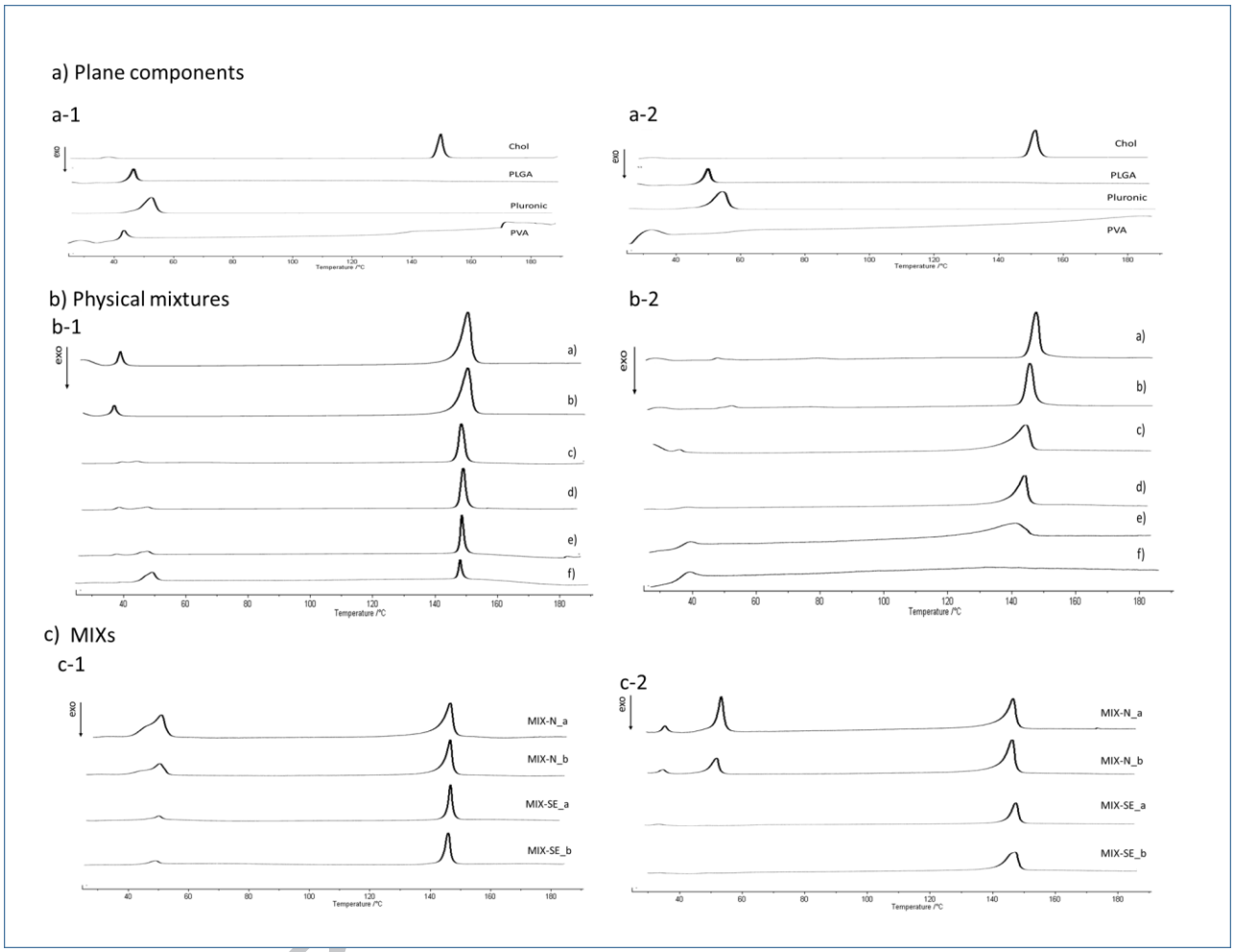

Fig. 2: DSC curves. ***(a)*** *plain components,* ***(b)*** *physical mixtures: Chol:PLGA 1:0.1w:w (line a), Chol:PLGA 1:0.25 (line b), Chol:PLGA 1:0.4 (line c), Chol:PLGA 1:1 (line d), Chol:PLGA 0.25:1 (line e), Chol:PLGA 0.1:1 (line f);* ***(c)*** *MIX Nps samples: MIX-N_a (line a); MIX-N_b (line b); MIX-SE_a (line c); MIX-SE_b (line d). All the samples underwent to two consecutive heating cycle: the first (**a-1, b-1, c-1**) reported in panel 1 (left) and the second (re-fusion) (**a-2, b-2, c-2**) reported in panel 2 (right).*

4.2.3 Nanoparticles stability

Stability of MIX-N and MIX-SE in PBS suspension stored at 4°C was monitored for 14 days by PCS analysis (change in diameter, monodispersion of samples, superficial charge) along with the possible loss of Chol, PLGA, and surfactant (**Fig. 3).**

MIX-N_a was stable in terms of both dimension and composition during the storage time. On the contrary, MIX-N_b changed both their dimension and composition: a trend in reduction of Z-Average was measured notwithstanding both PDI and D90 increased during the experimental time (the value of D(90) shifts from 503 to 708 nm, see supplementary data for size distribution, **Fig. S2**). The amount of Chol in MIX-N_b was

reduced from 65±2% at the day 0 to 46±1% at the day 14. Chol, probably not well integrated into the structure, was lost inducing a change in Chol-PLGA reorganization which reflect the major heterogeneity in size of MIX_N_b.

Both MIXs-SE_a and MIXs-SE_b showed a higher stability after the 14 days of storage as both physico-chemical and composition data did not show remarkable modifications (**Figure 3**).

For both kind of MIXs, samples prepared with a mixture Chol:PLGA 1:1 (MIX-N_a and MIX_ES_a) were also analyzed for their chemical stability after incubation in a complex medium composed by PBS and FBS (50%). The amount of Chol was mainly constant within 6 hours (see supplementary Table S2); minimum losses were detectable (less than 10% of total Chol), suggesting that Chol is stable enclosed into matrix structure and that its release during the circulation should happen at very low extent.

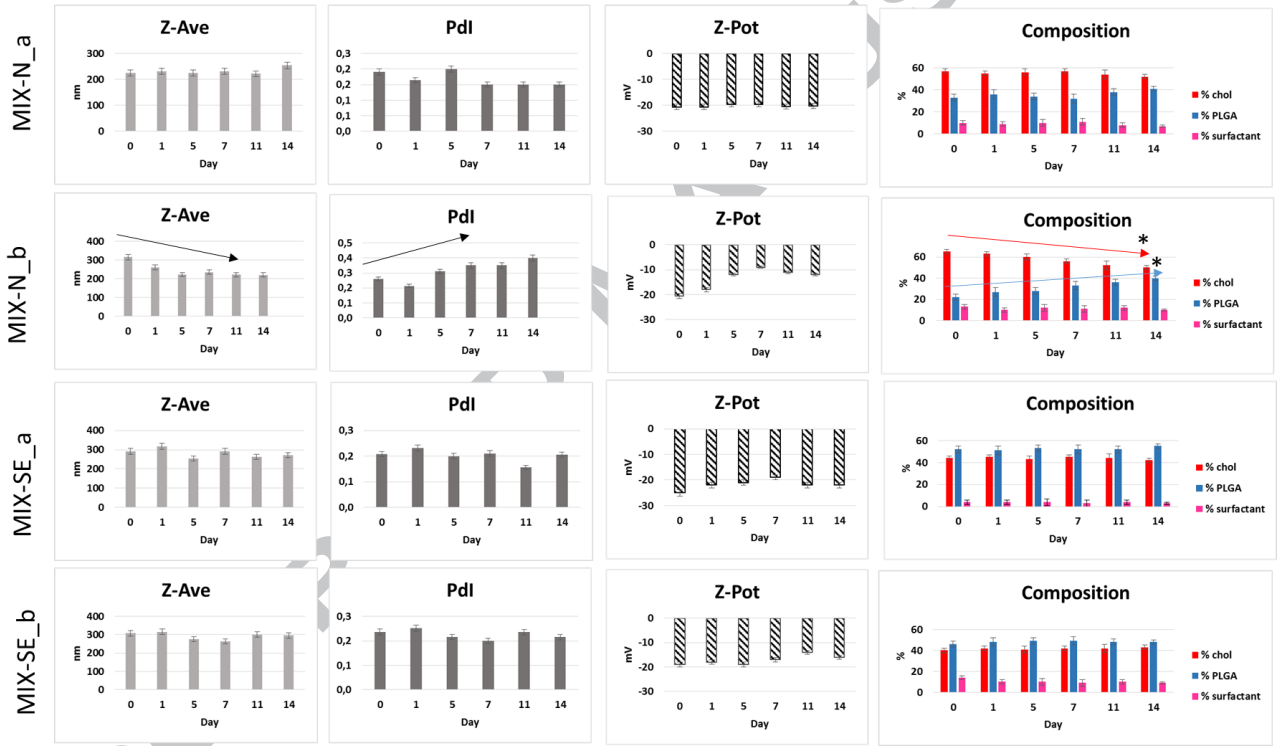

Fig. 3: Physico-chemical characterization and composition of MIX NPs. MIX-N_a, MIX-N_b, MIX-SE_a and MIX-SE_b during 14 days of storage.

4.3 Biological studies on MIX-N_a and MIX- SE_a *in vitro*:

As MIX-N_a and MIX- SE_a showed dimensions suitable for i.p. administration, stable reorganization of both Chol and PLGA, and suitable stability, they were selected for *in vitro* studies. To deliver Chol into the CNS, the surface of MIX NPs was modified with a g7 peptide able to induce the BBB crossing (Tosi et al., 2007; Tosi et al., 2011b) (g7-MIX-N_a and g7-MIX-SE_a). Moreover, a rhodamine fluorescent label was bound to the surface to trace the MIX NPs in cells and tissues (g7-(Rhod)-MIX-N_a and g7-(Rhod)-MIX-

SE_a). For physico-chemical characterization of g7-MIX-N_a, g7-MIX-SE_a, g7-(Rhod)-MIX-N_a, and g7-(Rhod)-MIX-SE_a see **supplementary data Table S3 and Fig. S3**.

4.3.1 Toxicity

Apoptosis induced by g7-MIX-N_a and g7-MIX-SE_a in primary neuronal cultures after 24 h of treatment was evaluated quantifying the levels of cleaved casapse-3 and cleaved PARP (**Fig. 4**). Cells treated with nanoparticles showed significantly higher levels of cleaved caspase-3 (that provides a read-out for apoptotic processes initiated within a cell) compared to control cells. Another key protein involved in cellular apoptosis is the nuclear enzyme poly(ADP-ribose), PARP. In particular, in case of severe damage, PARP can be cleaved by enzymes such as caspases or cathepsins that inactivate the protein, promoting apoptosis (Virág et al., 2013). In both cell line, levels of cleaved PARP were not significanlty altered regardless the MIX-NPs tested. Since PARP is downstream of caspase-3, the increase in cleaved caspase-3 might not be sufficient to trigger apoptotic events via PARP.

These data were confirmed on cellular level using immunocytochemistry as read-out. Neuronal cells were treated for 6–24 hours with g7-MIX-N_a and g7-MIX-SE_a, and the fraction of apoptotic cells was assessed and compared to untreated control cells (**Fig. 4-c**) showing that no major apoptotic processes are active upon application of g7-samples.

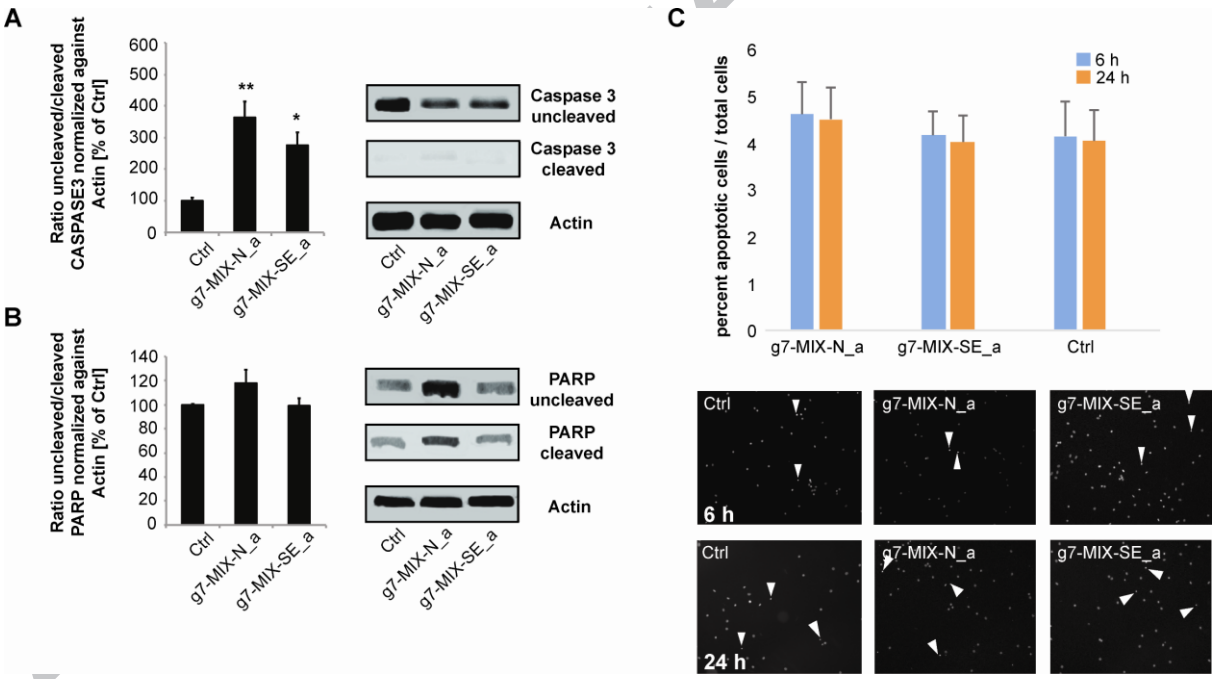

Fig4: Toxicity of MIX NPs. A,B) Quantification of the ratio between (A) uncleaved and cleaved Caspase 3 normalized to Actin and (B) between uncleaved and cleaved PARP normalized to Actin (n = 3 per condition). Exemplary WB bands are shown on the right. C) Evaluation of 10 optic fields of view per condition regarding the total number of cells (labeled by Hoechst33342) and percent apoptotic cells (labeled by FITC Annexin V).

4.3.2 *In vitro* uptake

To study both cellular uptake and localization, g7-(Rhod)-MIX-N_a and g7-(Rhod)-MIX-SE_a were applied to glial-neuronal co-cultures. MIX-NPs are visualized as red fluorescent puncta. We observed that both

samples (g7-(Rhod)-MIX-N_a and g7-(Rhod)-MIX-SE_a) were efficiently taken up by both neurons and glial cells. Already after 6 h of treatment, both neurons and glial cells showed uptake of MIX NPs in similar amount (**Fig.5 panel a**).

To provide information about the mechanism of internalization we investigated the amount of nanoparticles co-localizing with caveolin (**Fig. 5 panel b**) or clathrin positive vesicles (**Fig. 5 panel c**) 6 and 24 h after application. The results showed that, on average, only about 5% of MIX-NPs co-localize with caveolin positive signals, while about 60% of MIX-NPs co-localized with clathrin positive signals, without any difference between g7-(Rhod)-MIX-N_a and g7-(Rhod)-MIX-SE_a. This association with clathrin positive signals did not significantly change during time (6 h and 24 h after transfection).

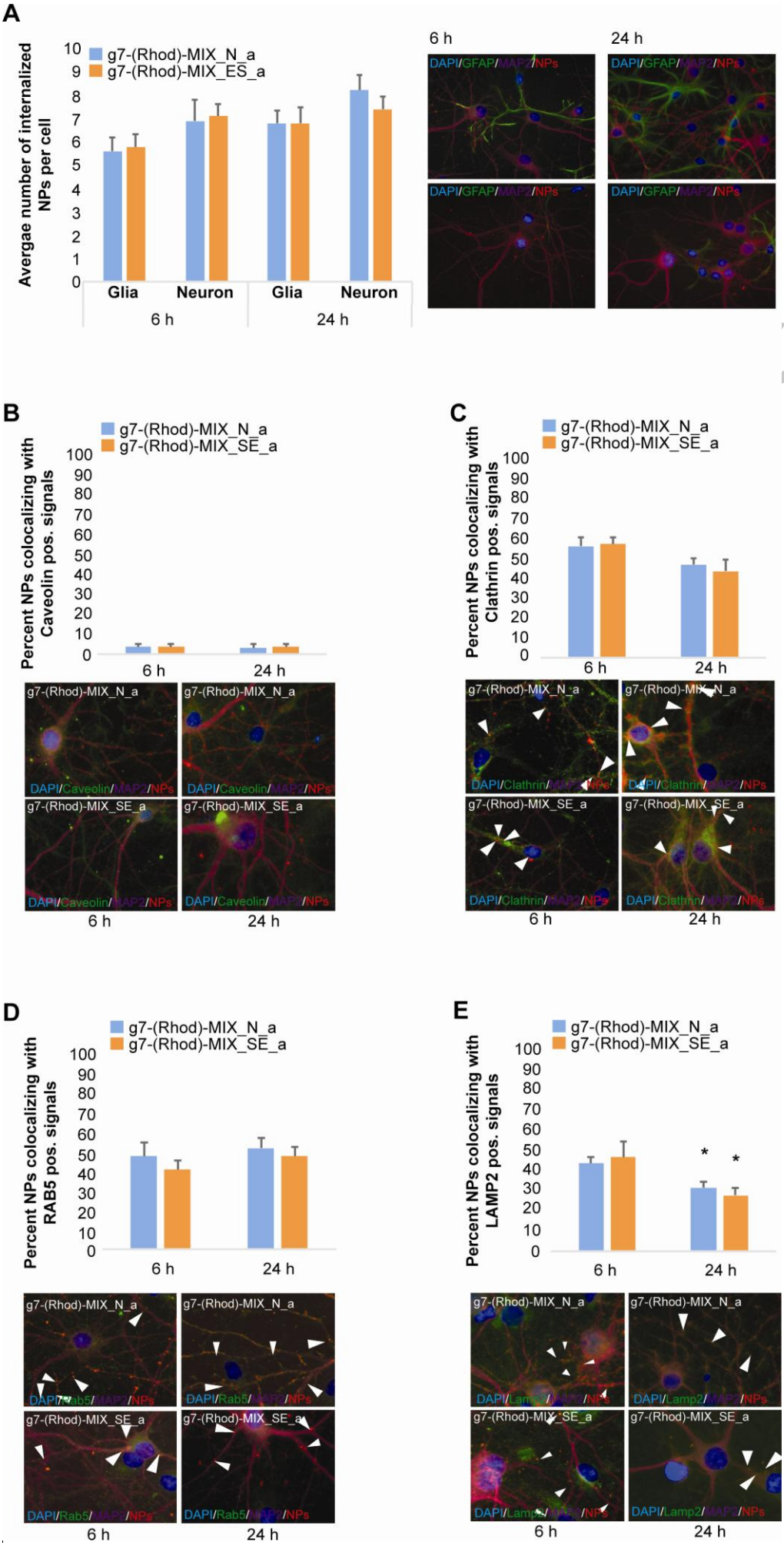
A
Avergae number of internalized NPs per cell
g7-(Rhod)-MIX_N_a
g7-(Rhod)-MIX_ES_a
Glia
Neuron
Glia
Neuron
6 h
24 h
6 h
24 h
DAPI/GFAP/MAP2/NPs
B
Percent NPs colocalizing with Caveolin pos. signals
g7-(Rhod)-MIX_N_a
g7-(Rhod)-MIX_SE_a
6 h
24 h
g7-(Rhod)-MIX_N_a
g7-(Rhod)-MIX_SE_a
DAPI/Caveolin/MAP2/NPs
C
Percent NPs colocalizing with Clathrin pos. signals
g7-(Rhod)-MIX_N_a
g7-(Rhod)-MIX_SE_a
6 h
24 h
DAPI/Clathrin/MAP2/NPs
D
Percent NPs colocalizing with RAB5 pos. signals
g7-(Rhod)-MIX_N_a
g7-(Rhod)-MIX_SE_a
6 h
24 h
DAPI/Rab5/MAP2/NPs
E
Percent NPs colocalizing with LAMP2 pos. signals
g7-(Rhod)-MIX_N_a
g7-(Rhod)-MIX_SE_a
*
*
6 h
24 h
DAPI/Lamp2/MAP2/NPs

Fig.5 Uptake of MIX NPs on hippocampal cells. A) Amount of MIX-NPs (red signal) co-localizing with GFAP, a marker for glial cells (green) and MAP2, a marker for neurons (magenta), assessed after 6 h and 24 h. Cell nuclei are visualized with DAPI (blue). The average number of MIX-NPs per cell (n = 10) is shown. B,C) Neurons were visualized by MAP2 staining and cell nuclei by DAPI. The amount of MIX-NPs (red signals) co-localizing with anti-Caveolin positive signals (B) and anti-Clathrin positive signals (C) was assessed (n = 10) 6 and 24 h after application of the MIX-NPs. D) MIX-NPs further co-localizing with Rab5, a marker for early endosomes. E) Both types of NP further show co-localization with LAMP2, a marker for lysosomes.

A co-localization of 60% between positive signals of MIX-NPs and Rab5 (located on the cytoplasmic surface of early endosomes) confirms the involvement of clathrin dependent endocytotic pathways during the cellular internalization for both types of MIX NPs (**Fig. 5, panel d**). As early endosomes often ultimately fuse with lysosomes within the cell, we finally investigated the co-localization of nanoparticles and LAMP2 (Lysosome-associated membrane protein 2), a marker for lysosomes. Images in **Fig. 5, panel E** clearly demonstrate the accumulation of MIX NPs in lysosomes. Indeed, both types of g7-(Rhod)-MIXs showed co-localization with LAMP2 6 h after treatment. Co-localization decreases 24 h after treatment (**Fig. 5 panel E**). It might be possible that some nanoparticles escape from endo/lysosomes into the cytoplasm, or that the number of lysosomes increases as a consequence of the stress caused by treatment with g7 MIX NPs. Therefore, we quantified the amount of LAMP2 and RAB5 positive vesicles per cell in cultures treated with both g7-(Rhod)-MIX-N_a and g7-(Rhod)-MIX-SE_a. The results show that the total number of vesicles (lysosomes and RAB5 positive vesicles) is even decreased 24 h after application of MIX-NPs. Correlating this data with the number of MIX Nps per cells which remained constant, we can hypothesized that some MIX-NPs may escape from lysosomes after 24 h of treatment (**Fig. 6**).

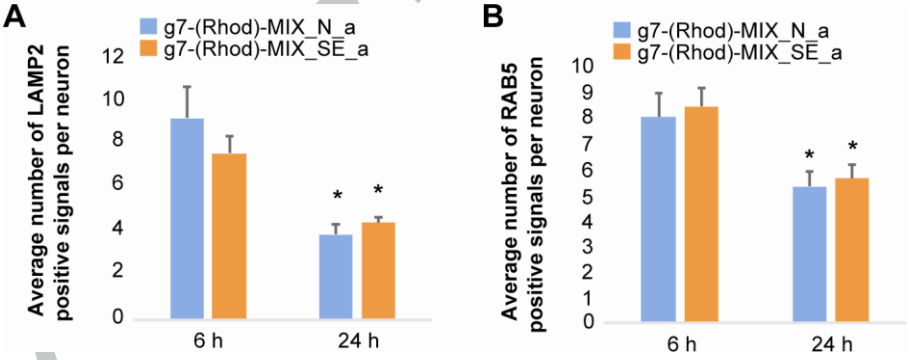

Fig. 6: Co-localization of MIX NPs with LAMP2 and RAB5. The average number of LAMP2 positive structures (lysosomes) (A) and RAB5 positive structures (endosomes) (B) per cell was evaluated 6 and 14 h after treatment with MIX-NPs by immunocytochemistry and quantified for 10 cells per condition.

4.2.3 Effect on excitatory synaptic receptors

Assuming that Chol is incorporated into cellular membranes, possibly changing lipid composition, we next wondered whether we are able to detect alterations in the physiology of neurons. Given that synaptic

transmission is a key function of neuronal cells and that lipid composition might be especially important at excitatory postsynaptic spines, we focused on the characterization of alterations after MIX NPs application at these synapses in hippocampal neurons. Even in the early stages of HD, MRI and postmortem studies have shown that pathology is widespread with several structures affected, including the hippocampus, a region known to be important for learning, memory and spatial navigation (Bird and Burgess, 2008; Rosas et al., 2003).

As proof of principle, we evaluated the composition of synaptic *N*-methyl-D-aspartate receptors (NMDAR) regarding the three major subunits (GluN1, GluN2A and GluN2B). NMDAR mediate synaptic plasticity and memory formation. After application of g7-MIX-N_a and g7-MIX-ES_a, an increase in GluN2B levels was observed after treatment (significant for g7-MIX-N_a, and as trend for g7-MIX-SE_a) (**Fig. 7**), along with a slight increase in GluN2A (significant for g7-MIX-SE_a). In turn, the synaptic levels of and GluN1 were significantly reduced after treatment with both types of MIX-NPs. Thus, the increase in GluN2A or N2B might not translate into an increase of functional receptors at the membrane, as functional NMDAR receptors will be formed of GluN1 together with either N2A or N2B. Nevertheless, this data shows that Chol was delivered by MIX NPs and was able to influence synapse composition by direct or indirect modes of action.

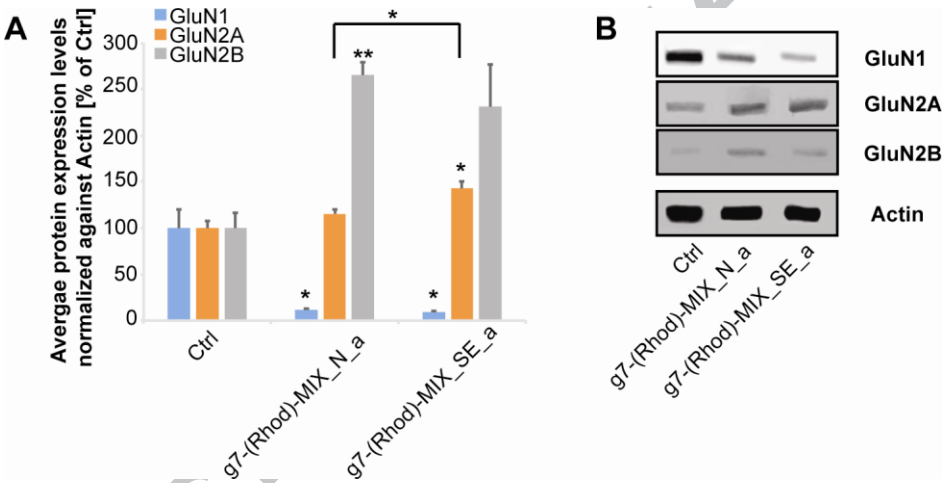

Fig.7: Effect of g7-MIX NPs on excitatory synaptic receptors. g7-MIX NPs were applied to primary hippocampal neurons and NMDAR subunits quantified by Western Blot experiments. Experiments were performed in triplicates. A) Western blot band intensities were quantified for the three major subunits of the NMDAR, GluN1, N2A and N2B, and the values normalized against Actin. B) Exemplary images of Western Blot bands.

5. DISCUSSION AND CONCLUSION:

In this study, we proposed hybrid lipid-polymer nanoparticles (MIX NPs) as strategy to stabilize high amounts of Chol, and to optimize its administration and application in HD therapy. In MIX NPs, Chol assumes at once the role of active ingredient and integral part of the carrier so that the polymer composing NPs (PLGA) can be reduced.

MIX NPs were formulated combining Chol and PLGA and by applying two easily up-scalable preparation techniques typically used in the rearrangement of hydrophobic materials, nanoprecipitation (MIX-N) and

single emulsion (MIX-SE). Unless is difficult to describe the internal structure of the nanometric systems, combining physical (dimension, surface charge), chemical (composition), morphological and stability studies, a different architecture of MIX NPs depending on the formulation technique can be proposed.
Our working hypothesis is based on the premise that surfactant (type and concentration) as the production protocol play a pivotal role in the final structure.
MIX-N was prepared applying the same method used in a previous study (Belletti et al., 2016) adding an acetonic solution of Chol/PLGA to a water dispersion of Pluronic F 68 (0.5% v/v at 45°C) reorganized in small micelles (Somasundaran, 2006; Tsui et al., 2008). As well described by Lannibois at al. (Lannibois et al., 1997) the competition between coalescence of hydrophobic material and adsorption of surfactants at the water–hydrophobic droplet interface governs the final size and the stability of nanoparticles formed during nanoprecipitation. We hypothesized that, the diffusion of acetone from the Chol-PLGA solution into the Pluronics micelles water phase induces the precipitation and the reorganization of all the three components – Chol, PLGA and Pluronics. Hence, Chol and PLGA are closely dispersed and Pluronic F68 could be solubilized into Chol for which it has a strong affinity (Maskarinec et al., 2002). The high residual amount of Pluronic F68 could justify the permeability of structure and the rapid release of Chol, with consequent destabilization of nanoparticles prevalently composed of Chol (see data on stability) the MIX-N_b, MIX-N_c and MIX-N_d (Chol:PLGA w/w ratio 1:0.4; 1:0.25; 1:0.1, respectively). Only MIX-N_a appeared stable during time; the high amount of PLGA mixed in formulation (Chol:PLGA w/w ratio 1:1) probably well guarantees a better mixed system architecture.
In MIX-SE preparation Pluronic F68 was replaced with PVA, a water dispersible polymer typically used to stabilize the emulsion (Dinarvand et al., 2011). The slow solvent evaporation induces the precipitation of the two major component PLGA and Chol according to the solubility or/and to the precipitation rate. Hence, the component cannot be closely dispersed. Therefore, the nanoparticle structure could be formed by a non-homogeneous core of Chol and PLGA regardless to the ratio of the two components surrounded by a PVA layer (Sahoo et al., 2002).

Independently from the preparation approaches (nanoprecipitation and single emulsion), Chol:PLGA ratio of 1:1 w:w was the most suitable composition whit respect to chemical physical composition, final Chol content, stability and yield of production, thus this sample was selected for further investigations.
Aiming to transport Chol into the brain, we engineered the surface of MIX NPs with g7, a peptide designed for BBB crossing. g7-MIX-N_a obtained by nanoprecipitation and g7-MIX-SE_a obtained by single emulsion, were tested *in vitro* using hippocampal cells. From a toxicological point of view, we did not observe enough cellular stress caused by MIXs to induce apoptotic pathways in cells or cause necrosis of cells. However, g7-MIX-N_a NPs, in which the sterol is probably more accessible and un-protected, slightly induced more cleavage of caspase-3 compared to g7-MIX-SE_a.
Interestingly, both samples followed the same pathway for cellular uptake, taking advantage mainly of clathrin-dependent mechanism. These findings strongly agree with previous published data describing the cellular interaction of g7-NP made only by PLGA (Vilella et al., 2015), suggesting that the presence of the targeting g7 than the surface composition (Chol-PLGA ratio) has a major effect on the nanoparticles-cell interaction. Moreover, both g7-MIX NPs showed the ability to escape from lysosomes to some extent, making Chol available for biological functions.
We then wanted to investigate if the different MIX-NPs reorganization was able to affect the cellular response focusing on NMDAR expression which is involved in the initial neuronal stress and dysfunction.
In fact, NMDAR-mediated excitotoxicity has been proposed to play a role HD and increased striatal NMDAR-mediated synaptic currents in YAC72, a mouse model for HD, compared to wild-type mice were reported (Li et al., 2003).

We observed that g7_MIX NPs induced some alterations in NMDAR which highlights effects of the delivered NPs at intracellular level, however, we detected slight differences in between the two types of g7 MIX-NPs on NMDAR composition, which confirmed that the different “architecture” may reflect minor differences in cellular interaction, even if it could influence the kinetic of drug-release. Based on this hypothesis, g7-MIX-SE NPs in which Chol should be more segregated into nanoparticles and released slowly, could be more useful for the modulation of the synaptic transmission in HD model.

This study through a combinatory approach that put together information from formulation, chemical physical characterization and in vitro test described a novel concept of “precision nanomedicine” specifically designed holding to mind the biological features of the pathology, relocating this concept from tumor to brain diseases. Chol that is deficient in HD brain was used not as a “simple active to encapsulate” but as a component of MIX–NPs targeted to the brain offering a unique non-invasive therapeutic option for restoring brain Chol deficiency. Further investigation in HD animal model will clarify the efficacy and the performance of this two kind of NPs opening the pave for innovative, intelligent treatment of HD.

Acknowledgments

The authors gratefully acknowledge the professional technical assistance of Dr. Massimo Tonelli and of Centro Grandi Strumenti, University of Modena and Reggio Emilia for his assistance in microscopical analysis ans Dr. Antonio Ballestrazzi for ESCA analyses.
This research was partially supported by UNIMORE grant FAR 2016 (PI Prof. Michele Zoli) and by Telethon grant 2017 (PI Prof Elena Cattaneo).

References:

Bach, D., Wachtel, E., 2003. Phospholipid/cholesterol model membranes: formation of cholesterol crystallites. Biochimica et Biophysica Acta (BBA)-Biomembranes 1610, 187-197.

Belletti, D., Grabrucker, A., Pederzoli, F., Menrath, I., Cappello, V., Vandelli, M., Forni, F., Tosi, G., Ruozi, B., 2016. Exploiting the versatility of cholesterol in nanoparticles formulation. International journal of pharmaceutics 511, 331-340.

Bettinetti, G., Mura, P., 1994. Dissolution properties of naproxen in combinations with polyvinylpyrrolidone. Drug development and industrial pharmacy 20, 1353-1366.

Bird, C.M., Burgess, N., 2008. The hippocampus and memory: insights from spatial processing. Nature Reviews Neuroscience 9, 182-194.

Block, R.C., Dorsey, E.R., Beck, C.A., Brenna, J.T., Shoulson, I., 2010. Altered cholesterol and fatty acid metabolism in Huntington disease. Journal of clinical lipidology 4, 17-23.

Chiou, W.L., Riegelman, S., 1971. Pharmaceutical applications of solid dispersion systems. Journal of pharmaceutical sciences 60, 1281-1302.

Dietschy, J.M., Turley, S.D., 2004. Thematic review series: brain Lipids. Cholesterol metabolism in the central nervous system during early development and in the mature animal. Journal of lipid research 45, 1375-1397.

Dinarvand, R., Sepehri, N., Manoochehri, S., Rouhani, H., Atyabi, F., 2011. Polylactide-co-glycolide nanoparticles for controlled delivery of anticancer agents. International journal of nanomedicine 6, 877.
Egerton, R.F., 2005. Physical principles of electron microscopy. Springer.

Gao, H., 2016. Progress and perspectives on targeting nanoparticles for brain drug delivery. Acta Pharm Sin B. 6, 268–286.

Grabrucker, A., Vaida, B., Bockmann, J., Boeckers, T.M., 2009. Synaptogenesis of hippocampal neurons in primary cell culture. Cell and tissue research 338, 333.

Joshi, D., Lan-Chun-Fung, Y., Pritchard, J., 1979. Determination of poly (vinyl alcohol) via its complex with boric acid and iodine. Analytica Chimica Acta 104, 153-160.

Kapoor, D.N., Bhatia, A., Kaur, R., Sharma, R., Kaur, G., Dhawan, S., 2015. PLGA: a unique polymer for drug delivery. Therapeutic delivery 6, 41-58.

Hersh, D.S., Wadajkar, A.S., Roberts, N., Perez, J.G., Connolly, N.P., Frenkel, V., Winkles, J.A., Woodworth, G.V., Kim, A.J., 2016. Evolving Drug Delivery Strategies to Overcome the Blood Brain Barrier. Curr Pharm Des. 22, 1177–1193.

Lannibois, H., Hasmy, A., Botet, R., Chariol, O.A., Cabane, B., 1997. Surfactant limited aggregation of hydrophobic molecules in water. Journal de Physique II 7, 319-342.

Leoni, V., Long, J.D., Mills, J.A., Di Donato, S., Paulsen, J.S., group, m.o.t.P.-H.s., 2013. Plasma 24S-hydroxycholesterol correlation with markers of Huntington disease progression. Neurobiology of disease 55, 37-43.

Li, L., Fan, M., Icton, C.D., Chen, N., Leavitt, B.R., Hayden, M.R., Murphy, T.H., Raymond, L.A., 2003. Role of NR2B-type NMDA receptors in selective neurodegeneration in Huntington disease. Neurobiology of aging 24, 1113-1121.

Maskarinec, S.A., Hannig, J., Lee, R.C., Lee, K.Y.C., 2002. Direct observation of poloxamer 188 insertion into lipid monolayers. Biophysical journal 82, 1453-1459.

Rosas, H., Koroshetz, W., Chen, Y., Skeuse, C., Vangel, M., Cudkowicz, M., Caplan, K., Marek, K., Seidman, L., Makris, N., 2003. Evidence for more widespread cerebral pathology in early HD An MRI-based morphometric analysis. Neurology 60, 1615-1620.

Sahoo, S.K., Panyam, J., Prabha, S., Labhasetwar, V., 2002. Residual polyvinyl alcohol associated with poly (D, L-lactide-co-glycolide) nanoparticles affects their physical properties and cellular uptake. Journal of controlled release 82, 105-114.

Saraiva, C.,, Praça, C., Ferreira, R., Santos, T., Ferreira, L., Bernardino, L., 2016. Nanoparticle-mediated brain drug delivery: Overcoming blood-brain barrier to treat neurodegenerative diseases. J Control Release 10, 235-234.

Schmeisser, M.J., Ey, E., Wegener, S., Bockmann, J., Stempel, A.V., Kuebler, A., Janssen, A.-L., Udvardi, P.T., Shiban, E., Spilker, C., 2012. Autistic-like behaviours and hyperactivity in mice lacking ProSAP1/Shank2. Nature 486, 256-260.

Somasundaran, P., 2006. Encyclopedia of surface and colloid science. CRC press.

Tosi, G., Costantino, L., Rivasi, F., Ruozi, B., Leo, E., Vergoni, A.V., Tacchi, R., Bertolini, A., Vandelli, M.A., Forni, F., 2007. Targeting the central nervous system: in vivo experiments with peptide-derivatized nanoparticles loaded with Loperamide and Rhodamine-123. Journal of controlled release 122, 1-9.

Tosi, G., Fano, R.A., Bondioli, L., Badiali, L., Benassi, R., Rivasi, F., Ruozi, B., Forni, F., Vandelli, M.A. 2011 a. Investigation on mechanisms of glycopeptide nanoparticles for drug delivery across the blood-brain barrier. Nanomedicine (Lond) 6, 423-436.

Tosi, G., Fano, R., Badiali, L., Bondioli, L., Ruozi, B., Vergoni, A., Rivasi, F., Benassi, R., Vandelli, M., Forni, F., 2011b. Nanoparticles for Brain Delivery of Drugs: In Vivo Experiments and Mechanism of Blood-Brain Barrier Crossing. American Journal of Neuroprotection and Neuroregeneration 3, 13-20.

Tsui, H.-W., Hsu, Y.-H., Wang, J.-H., Chen, L.-J., 2008. Novel behavior of heat of micellization of Pluronics F68 and F88 in aqueous solutions. Langmuir 24, 13858-13862.

Valenza, M., Carroll, J.B., Leoni, V., Bertram, L.N., Björkhem, I., Singaraja, R.R., Di Donato, S., Lutjohann, D., Hayden, M.R., Cattaneo, E., 2007. Cholesterol biosynthesis pathway is disturbed in YAC128 mice and is modulated by huntingtin mutation. Human molecular genetics 16, 2187-2198.

Valenza, M., Chen, J.Y., Di Paolo, E., Ruozi, B., Belletti, D., Ferrari Bardile, C., Leoni, V., Caccia, C., Brilli, E., Di Donato, S., Boido, M.M., Vercelli, A., Vandelli, M.A., Forni, F., Cepeda, C., Levine, M.S., Tosi, G., Cattaneo, E., 2015. Cholesterol-loaded nanoparticles ameliorate synaptic and cognitive function in Huntington's disease mice. EMBO Molecular Medicine 7, 1547-1564.

Valenza, M., Leoni, V., Karasinska, J.M., Petricca, L., Fan, J., Carroll, J., Pouladi, M.A., Fossale, E., Nguyen, H.P., Riess, O., 2010. Cholesterol defect is marked across multiple rodent models of Huntington's disease and is manifest in astrocytes. Journal of Neuroscience 30, 10844-10850.

Vilella, A., Ruozi, B., Belletti, D., Pederzoli, F., Galliani, M., Semeghini, V., Forni, F., Zoli, M., Vandelli, M.A., Tosi, G., 2015. Endocytosis of nanomedicines: the case of glycopeptide engineered PLGA nanoparticles. Pharmaceutics 7, 74-89.

Virág, L., Robaszkiewicz, A., Rodriguez-Vargas, J.M., Oliver, F.J., 2013. Poly (ADP-ribose) signaling in cell death. Molecular aspects of medicine 34, 1153-1167.

Zuccato, C., Valenza, M., Cattaneo, E., 2010. Molecular Mechanisms and Potential Therapeutical Targets in Huntington's Disease. Physiological Reviews 90, 905-981.

Supplementary data

Hybrid nanoparticles as a new technological approach to enhance CNS delivery of cholesterol into the brain

Belletti Daniela[1], Grabrucker Andreas[2,3], Pederzoli Francesca[1], Menerath Isabel[4], Vandelli Maria Angela[1], Tosi Giovanni[1], Duskey Thomas Jason[1], Forni Flavio[1], Ruozi Barbara[1#]

Supplementary

TableS1: Schematic representation of the samples formulated

Chol:PLGA (w/w)	Chol	PLGA			Method	Name	Use
	mg Chol	mg PLGA-COOH	mg PLGA-g7	mg PLGA-rhod			
0:1		50			Nanoprecipitation	NP-N	physico-chemical/technological characterization
1:1	25	25				MIX-N_a	physico-chemical/technological characterization
1:1	25	22.5	2.5			g7-MIX-N_a	In vitro study (toxicity)
1:1	25	21.3	2.5	1.2		g7-(Rhod-)MIX-N_a	In vitro study (uptake)
1:0.4	35.5	15.5				MIX-N_b	physico-chemical/technological characterization
1:0.25	40	10				MIX-N_c	physico-chemical/technological characterization
1:0.1	45	5				MIX-N_d	physico-chemical/technological characterization
0:1		50			Single emulsion	NP-SE	physico-chemical/technological characterization
1:1	25	25				MIX- SE _a	physico-chemical/technological characterization
1:1	25	22.5	2.5			g7-MIX-SE_a	In vitro study (toxicity)
1:1	25	21.3	2.5	1.2		g7-(Rhod)-MIX-SE _a	In vitro study (uptake)

1:0.4	35.5	15.5				MIX-SE_b	physico-chemical/technological characterization
1:0.25	40	10				MIX-SE_c	physico-chemical/technological characterization
1:0.1	45	5				MIX-SE_d	physico-chemical/technological characterization

FIG S1: DSC analyses

			I° (<40°C)		II° (41-100°C)		III° (>100°C)	
			Tonset (°C) [S.D]	Area (J/g) [S.D]	Tonset (°C) [S.D]	Area (J/g) [S.D]	Tonset (°C) [S.D]	Area (J/g) [S.D]
plain components	PLGA	first			47.2 [2.1]	15.2 [0.5]		
		second			45.0 [1.2]	13.9 [0.4]		
	CHOL	first	38.1 [1.1]	6.8 [0.9]			151.0 [2.1]	47.0 [0.5]
		second					150.0 [1.5]	47.2 [0.4]
	PVA	first	31.7 [1.2]	4.9 [0.8]				
		second						
	Pluronic	first			51.2 [1.0]	81.0 [1.0]		
		second			50.1 [0.9]	70.9[0.4]		
physical mixtures	a	first	31.2 [1.2]	6.1 [1.1]			144.1 [0.8]	46.9 [1.2]
		second	35.5 [0.3]	2.7 [0.4]			143.0 [0.8]	51.6 [1.2]
	b	first	31.2 [0.7]	4.9 [0.9]			144.2 [1.5]	46.9 [0.5]
		second	37.9 [0.8]	3.7 [1.2]			143.8 [1.2]	46.8 [0,7]
	c	first	36.2 [1.2]	0.7 [1.2]	40.8 [0.5]	1.2 [0.7]	145.3 [1.8]	41.0 [1,0]
		second	37.3 [1.8]	0.7 [0.3]			137.2 [0.3]	27.9 [1.1]
	d	first	36.1 [0.7]	1.7 [0.5]	43.6 [1.1]	3.6 [0.5]	147.6 [1.5]	32.1 [0.8]
		second	37.2 [0.5]	0.8 [0.5]			142.8 [1.2	22.1 [0.9]
	e	first	36.0 [1.0]	0.6 [0.1]	43.1 [0.9]	2.6 [0.4]	147.6 [1.2]	16.2 [0.7]
		second	37.4 [0.3]	0.8 [0.1]			126.4 [0.4]	8.4 [0.3]
	f	first	36.2 [1.2]	0.1	42.9 [0.6]	4.5 [0.5]	146.9 [1.1]	3.7 [0.3]
		second	36.1 [0.4]	1.1 [0,2]				
samples	MIX-N_a	first					142.9 [1,1]	20.8 [0.6]
		second	30.6 [0.2]	1.8 [0.2]	48.7 [0.7]	11.4 [0.8]	142.5 [1.2]	19.5 [0.4]
	MIX-N_b	first					144.7 [1.3]	31.5 [0.5]
		second	29.7 [0.7]	1.8 [0.5]	45.6 [0.5]	10.7 [0.5]	142.3 [0.5]	29.7 [0.9]
	MIX-SE_a	first			48.9 [1.2]	3.7 [0.3]	147.5 [0.5]	24.6 [0.9]
		second					141.2 [1.9]	19.8 [0.4]
	MIX-SE_b	first			46.2 [0.7]	5.4 [0.2]	147.6 [1.4]	26.6 [1.2]
		second					144.7 [1.8]	22.2[0.5]

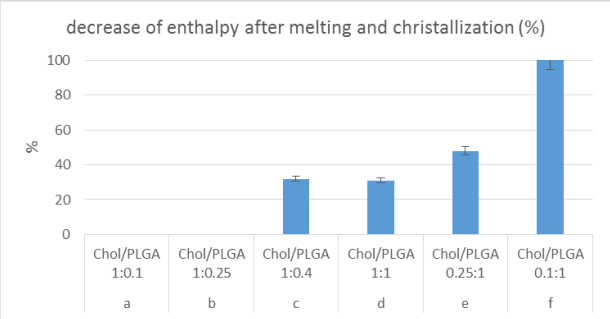

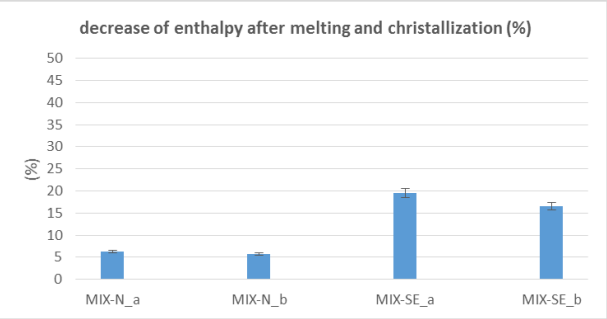

Data of DSC of plane components, physical mixtures and samples. Data in table refer to the first heating cycle and to the second re-heating that occurs after a controlled cooling. For each run onset and related area of transition were reported; in the histograms we reported analyses of the decreasing of enthalpy associated with Chol melting after first eating and cooling cycle

FIG S2: size distribution

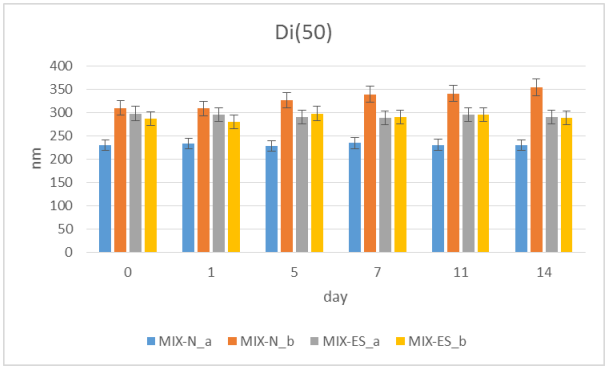

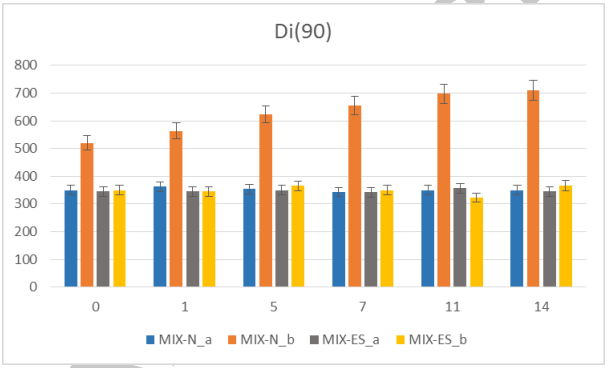

Table S2: Chol content in MIX-N_a and MIX-ES_a after incubation in PBS added of FBS (50% v/v) at 37°C. After incubation, samples were purified by centrifugation and nanoparticles analyzed for the Chol content as reported in methods section.

Sample	*Content of Chol (%) T0*	*Content of Chol (%) T 6h*
MIX-N_a	*38 ± 5*	*32± 3*
MIX-ES_a	*44 ± 2*	*41 ± 5*

Table S3: Physico-chemico characterization of modified samples used for *in vitro* study

Sample	Z-Ave (±SD) [nm]	PDI (±SD)	D90 (±SD) [nm]	Z-Pot (±SD)	% Chol	% PLGA	% surfactant.
g7-MIX-N_a	235 (±9)	0,26 (±0,02)	518 (±33)	-25 (±3)	33 (±11)	55 (±9)	12 (±2)
g7-(rhod)MIX-N_a	225 (±11)	0,22 (±0,03)	505 (±24)	-21 (±2)	34 (±4)	56 (±7)	8 (±1)
g7-MIX-SE_a	278 (±15)	0,16 (±0,01)	471 (±14)	-23 (±4)	45 (±3)	51 (±4)	4 (±1)

g7-(rhod)MIX-SE_a	2911 (±21)	0,19 (±0,03)	489 (±18)	-20 (±1)	43 (±2)	54 (±2)	3 (±1)

FIG. S3: ESCA analyses

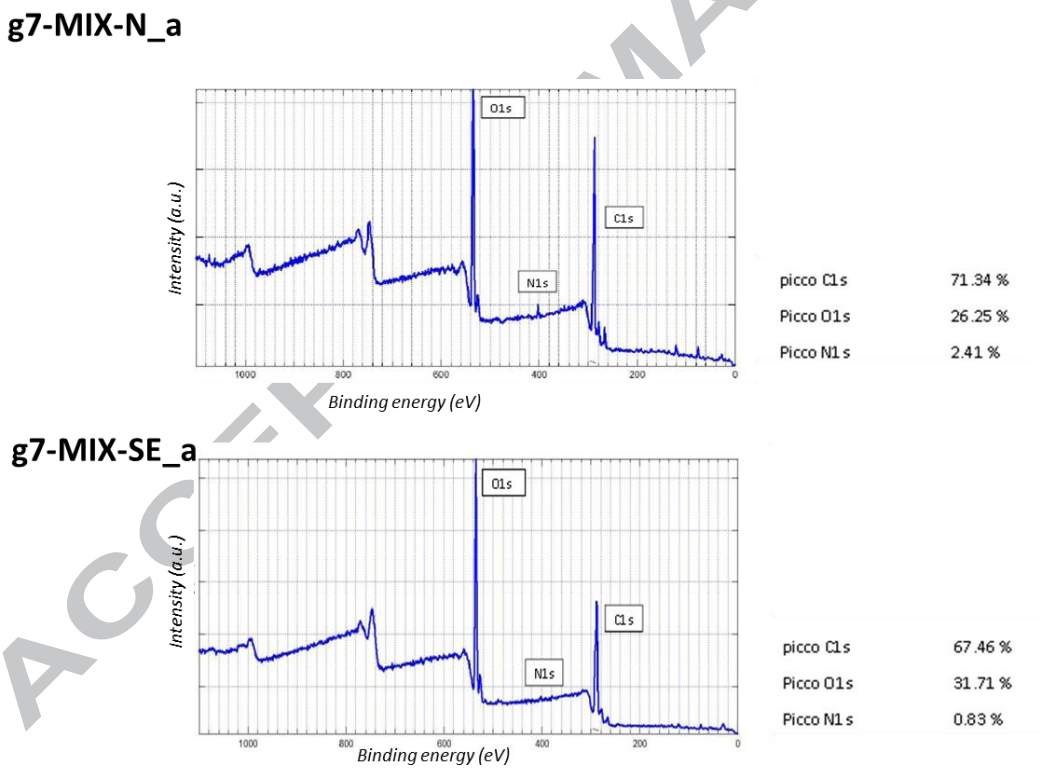

The presence of g7 on NPs surface was demonstrated by electron spectroscopy for chemical analysis (ESCA), showing the presence of nitrogen atoms on the surface of engineered NPs. ESCA was performed on a XRC 1000 X-ray source analysis system (Specs Surface Nano Analysis, Germany) and a Phoibos 150 hemispherical electron analyzer (Specs Surface Nano Analysis, Germany), using MgKα1,2 radiations. Spectra were recorded in fixed retardation ratio (FAT) mode with 40 eV pass energy. The pressure in the sample analysis chamber was around 10−9 mbar. Data were acquired and processed using the SpecsLab2 software.

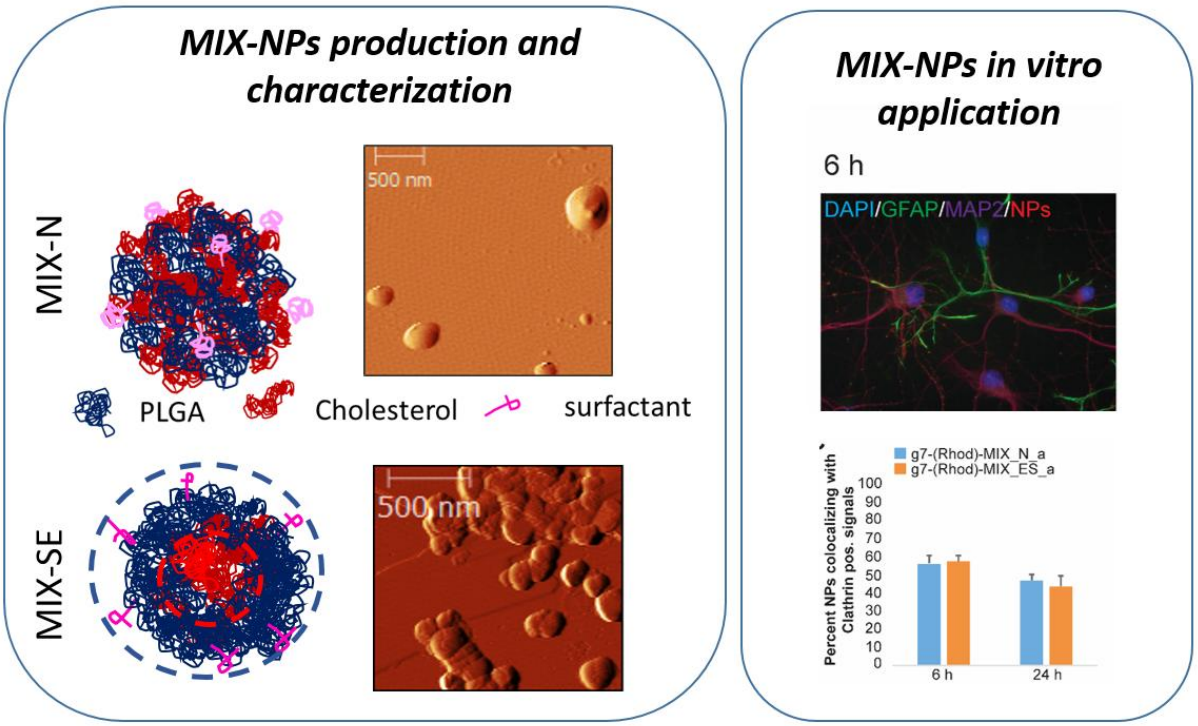
MIX-NPs production and characterization
MIX-N
500 nm
PLGA
Cholesterol
surfactant
MIX-SE
500 nm
MIX-NPs in vitro application
6 h
DAPI/GFAP/MAP2/NPs
g7-(Rhod)-MIX_N_a
g7-(Rhod)-MIX_ES_a
Percent NPs colocalizing with Clathrin pos. signals
100
90
80
70
60
50
40
30
20
10
0
6 h
24 h